

---

# CAMTUNER: REINFORCEMENT-LEARNING BASED SYSTEM FOR CAMERA PARAMETER TUNING TO ENHANCE ANALYTICS

---

Sibendu Paul<sup>1</sup> Kunal Rao<sup>2</sup> Giuseppe Coviello<sup>2</sup> Murugan Sankaradas<sup>2</sup> Oliver Po<sup>2</sup> Y. Charlie Hu<sup>1</sup>  
Srimat Chakradhar<sup>2</sup>

## ABSTRACT

Video analytics systems critically rely on video cameras, which capture high-quality video frames, to achieve high analytics accuracy. Although modern video cameras often expose tens of configurable parameter settings that can be set by end-users, deployment of surveillance cameras today often uses a fixed set of parameter settings because the end-users lack the skill or understanding to reconfigure these parameters.

In this paper, we first show that in a typical surveillance camera deployment, environmental condition changes can significantly affect the accuracy of analytics units such as person detection, face detection and face recognition, and how such adverse impact can be mitigated by dynamically adjusting camera settings. We then propose CAMTUNER, a framework that can be easily applied to an existing video analytics pipeline (VAP) to enable automatic and dynamic adaptation of complex camera settings to changing environmental conditions, and autonomously optimize the accuracy of analytics units (AUs) in the VAP. CAMTUNER is based on SARSA reinforcement learning (RL) and it incorporates two novel components: a light-weight analytics quality estimator and a virtual camera.

CAMTUNER is implemented in a system with AXIS surveillance cameras and several VAPs (with various AUs) that processed day-long customer videos captured at airport entrances. Our evaluations show that CAMTUNER can adapt quickly to changing environments. We compared CAMTUNER with two alternative approaches where either static camera settings were used, or a *strawman* approach where camera settings were manually changed every hour (based on human perception of quality). We observed that for the face detection and person detection AUs, CAMTUNER is able to achieve up to 13.8% and 9.2% higher accuracy, respectively, compared to the best of the two approaches (average improvement of  $\sim 8\%$  for both face detection and person detection AUs). When two cameras are deployed side-by-side in a real world setting (where one camera is managed by CAMTUNER, and the other is not), and video streams are sent over a 5G network, our dynamic tuning approach improves the accuracy of AUs by 11.7%. Also, CAMTUNER does not incur any additional delay in the VAP. Although we demonstrate use of CAMTUNER for remote and dynamic tuning of camera settings over a 5G network, CAMTUNER is lightweight and it can be deployed and run on small form-factor IoT devices. We also show that our virtual camera abstraction speeds up the RL training phase by 14X.

## 1 INTRODUCTION

Significant progress in machine learning and computer vision techniques in recent years for processing video streams (Krizhevsky et al., 2012), along with growth in Internet of Things (IoT), edge computing and high-bandwidth ac-

cess networks such as 5G (Qualcomm, 2019; CNET, 2019) have led to the wide adoption of video analytics systems. Such systems deploy cameras throughout the world to support diverse applications in entertainment, health-care, retail, automotive, transportation, home automation, safety, and security market segments. The global video analytics market is estimated to grow from \$5 billion in 2020 to \$21 billion by 2027, at a CAGR of 22.70% (Gaikwad & Rake, 2021).

A typical video analytics system consists of a video analytics pipeline (VAP) that starts with a camera capturing live feed of the target environment which is sent wirelessly to a server in the edge cloud running video analytics tasks such as face detection, as shown in Figure 1. Video analytics systems critically rely on the video cameras to capture high-quality

---

<sup>1</sup>Purdue University, West Lafayette, USA <sup>2</sup>NEC Laboratories America, New Jersey, USA. Correspondence to: Sibendu Paul <paul90@purdue.edu>, Kunal Rao <kunal@nec-labs.com>, Giuseppe Coviello <giuseppe.coviello@nec-labs.com>, Murugan Sankaradas <murugs@nec-labs.com>, Oliver Po <oliver@nec-labs.com>, Y. Charlie Hu <ychu@purdue.edu>, Srimat Chakradhar <chak@nec-labs.com>.

video frames, which are key to achieving high analytics accuracy.

We observe that although modern video cameras typically expose tens of configurable parameter settings (*e.g.*, brightness, contrast, sharpness, gamma, and acutance) via programmable APIs that can be used by end-users or applications to dynamically adjust the quality of the video feed, deployments of surveillance cameras today often use a fixed set of parameter settings (*e.g.*, the default settings provided by the manufacturer) because end-users lack the skill or understanding to appropriately change these parameters for different video analytics tasks or environments.

In this paper, we first conduct a measurement study to show that in a typical surveillance camera deployment, environmental condition changes can significantly affect the accuracy of analytics units (AUs) such as person detection, face detection and face recognition. Then, we show how such negative impact can potentially be mitigated by dynamically adjusting the settings of the camera.

Motivated by our findings above, we propose CAMTUNER, a framework that can be easily applied to any existing VAP to enable automatic and dynamic adaptation of the complex settings of the camera (in response to changing environmental conditions) to improve the accuracy of the VAP.

Designing such an automatic camera parameter tuning system has several challenges. Camera parameter tuning requires learning the best parameter settings for all possible environmental conditions, which is impossible to do offline for at least two reasons. (1) Since the environment for a particular camera is unknown before deployment, learning camera parameter tuning before deployment would require training for a huge space of possible deployment environments. (2) Due to the large number of combinations of camera parameter settings (*e.g.*, about 14K even for the four parameters we consider in this study), offline learning even for a particular deployment can take a very long time.

To address this challenge, CAMTUNER uses online reinforcement learning (RL) (Sutton et al., 1998) to continuously learn the best camera settings that would enhance the accuracy of the AUs in the VAP. In particular, CAMTUNER uses SARSA (Wiering & Schmidhuber, 1998), which is faster to train and achieves slightly better accuracy than Q-learning, which is another popular RL algorithm.

While RL is a fairly standard technique, applying it to tuning camera parameters in a real-time video analytics system poses two unique challenges.

First, implementing online RL requires knowing the reward/penalty for every action taken during exploration and during exploitation. Since no ground truth for an AU task like face detection is available during online operation of a

VAP, calculating the reward/penalty due to an action taken by an RL agent is a key challenge. To address this challenge, we propose an *AU-specific analytics quality estimator* that can accurately estimate the accuracy of the AU. Our estimator is light-weight, and it can run on a low-end PC or a simple IoT device to process video streams in real time.

Second, bespoke online RL learning at each camera deployment setup requires initial RL training, which can potentially take a long time for two reasons: (1) capturing the environmental condition changes such as the time-of-the-day effect can take a long time, and (2) taking an action on the real camera (*i.e.*, changing camera parameter settings) incurs a significant delay of about 200 ms. This limits the speed of state transitions, and hence the learning speed of RL, to about 5 changes (actions) per second. To address these two sources of delay, we propose a novel concept called *virtual camera*. A virtual camera mimics the effect of parameter setting changes on the frame capture of a real camera in software and thus has two key benefits over a physical camera: (1) it can complete an action of “camera setting change” almost instantaneously; and (2) it can augment a single frame captured by the real camera with many new transformed frames as if they were captured by the real camera but under different camera parameter settings. These two benefits allow the RL agent to explore actions at a much faster rate than using a real camera which drastically reduces the initial RL training time upon camera deployment.

CAMTUNER is implemented in a system with AXIS surveillance cameras and several VAPs (with various AUs) that processed day-long customer videos captured at airport entrances. Our evaluations show that CAMTUNER can adapt quickly to changing environments. We compared CAMTUNER with two alternative approaches where either static camera settings were used, or a *strawman* approach where camera settings were manually changed every hour (based on human perception of quality). We observed that for the face detection and person detection AUs, CAMTUNER is able to achieve up to 13.8% and 9.2% higher accuracy, respectively, compared to the best of the two approaches (average improvement of  $\sim 8\%$  for both face detection and person detection AUs). When two cameras are deployed side-by-side in a real world setting (where one camera is managed by CAMTUNER, and the other is not), and video streams are sent over a 5G network, our dynamic tuning approach improves the accuracy of AUs by 11.7%. Also, CAMTUNER does not incur any additional delay in the VAP. Although we demonstrate use of CAMTUNER for remote and dynamic tuning of camera settings over a 5G network, CAMTUNER is lightweight and it can be deployed and run on small form-factor IoT devices. We also show that our virtual camera abstraction speeds up the RL training phase by 14X.

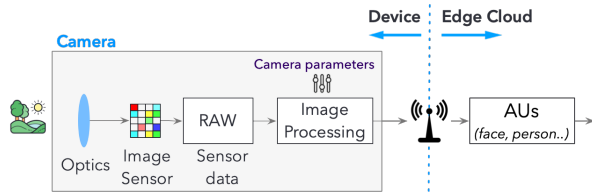


Figure 1. Video analytics pipeline

In summary, this paper makes the following contributions:

- We show that environmental condition changes can have a significant negative impact on the accuracy of AUs in video analytics pipelines, but the negative impact can be mitigated by dynamically adjusting the built-in camera parameter settings.
- We develop, to our knowledge the first system, that automatically and adaptively learns the best settings for cameras deployed in the field in reaction to environmental condition changes to improve the AU accuracy.
- We present two novel techniques that make the RL-based camera-parameter-tuning design feasible: a light-weight analytics quality estimator that enables online RL without ground truth, and a virtual camera that enables fast initial RL training.
- We experimentally show that compared to static and strawman approach, CAMTUNER achieves up to 13.8% and 9.2% higher accuracy for face detection and person detection AU, respectively, while incurring no extra delay to the AU pipeline. Our dynamic tuning approach also results in up to 11.7% improvement in accuracy of face-detection AU in a real-world deployment (video surveillance over 5G infrastructure).

## 2 BACKGROUND

Figure 1 also shows the image signal processing (ISP) pipeline within a camera. Photons from the external world reach the image sensor through an optical lens. The image sensor uses a Bayer filter (Bayer, 1976) to create raw-image data, which is further enhanced by a variety of image processing techniques such as demosaicing, denoising, white-balance, color-correction, sharpening and image compression (JPEG/PNG or video compression using H.264 (x26, 2021), VP9 (vp9, 2017), MJPEG, *etc.*) in the image-signal processing (ISP) stage (Ramanath et al., 2005) before the camera outputs an image or a video of frames.

The camera capture forms the initial stage of the VAP, which may include a wide variety of analytics tasks such as face detection, face recognition, human pose estimation, and license plate recognition.

In this paper, we study video analytics applications that are based on surveillance cameras. Such cameras are running 24X7 in contrast to DSLR, point-and-shoot or mobile cameras that capture videos on-demand. Popular IP video surveillance cameras are manufactured by vendors

such as AXIS (Communication), Cisco (CISCO), and Panasonic (i PRO). These surveillance camera manufacturers have exposed many camera parameters that can be set by applications to control the image generation process, which in turn affects the quality of the produced image or video. The exposed parameters include those for changing the amount of light that hits the sensor, the zoom level and field-of-view (FoV) at the image-sensor stage, and those for changing the color-saturation, brightness, contrast, sharpness, gamma, acutance, *etc.* in the ISP stage. Table 3 in Appendix A1 lists the parameters exposed by a few popular surveillance cameras in the market today.

## 3 MOTIVATION

We motivate the need for automatic, dynamic camera setting by experimentally showing the impact of environmental changes on AU accuracy when static and fixed camera settings are used, and the impact of dynamic camera settings on AU accuracy under the same environmental conditions. In addition, we also motivate the need for automatic, dynamic tuning of camera settings by experimentally showing that post-capture image transformations are not enough and they do not achieve the same high accuracy that is possible by directly tuning the camera settings.

### 3.1 Impact of Environment Change on AU Accuracy

Environmental changes happen for at least three reasons. First, such changes can be induced due to the change of the Sun’s movement throughout a day, *e.g.*, sunrise and sunset. Second, they can be triggered by changes in weather conditions, *e.g.*, rain, fog, and snow. Third, even for the same weather condition at exactly the same time of the day, the videos captured by the cameras at different deployment sites (*e.g.*, parking lot, factory, shopping mall, and airport) can have diverse content and ambient lighting conditions.

To illustrate the impact of environmental changes on image quality, and consequently on the accuracy of AUs, we experimentally measure the accuracy of two popular AUs (face detection and person detection) throughout a 24-hour (one-day) period. Since there are no publicly available video datasets that capture the environmental variations in a day or a week by using the same camera (at the same location), we use several proprietary videos provided by our customers. These videos were captured outside airports and baseball stadiums by stationary surveillance cameras, and we have labeled ground-truth information for several analytics tasks including face detection and person detection.

We use RetinaNet (Deng et al., 2019) for face detection and EfficientDet-v8 (Tan et al., 2020) for person detection. We compute the mean Average Precision (mAP) by using pycocotools (cocopai github).

Figure 2a shows that the average mAP values for the face

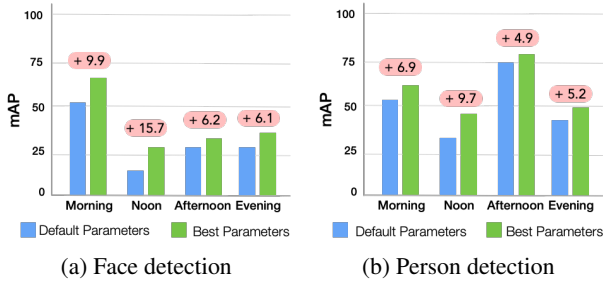


Figure 2. AU accuracy variation in a day and impact of camera settings.

detection AU during four different time periods of the day (morning 8AM - 10AM, noon 12PM - 2PM, afternoon 3PM - 5PM, and evening 6PM - 8PM), and with the default camera parameter settings, can vary by up to 40% as the day progresses (blue bars). Similarly, Figure 2b shows that the average mAP values for the person detection AU (with default camera parameter settings) can vary by up to 24% during the four time periods. These results show that changes in environmental conditions can adversely affect the quality of the frames retrieved from the camera, and consequently adversely impact the accuracy of the insights that are derived from the video data.

### 3.2 Impact of Camera Settings on AU Accuracy

To illustrate the impact of camera settings on AU accuracy, we consider four popular parameters that are common to almost all cameras: *brightness*, *contrast*, *color-saturation* (also known as *colorfulness*), and *sharpness*.

**Methodology:** Analyzing the impact of camera settings on video analytics is a significant challenge: it requires applying different camera parameter settings to the same input scene and measuring the resulting accuracy of insights from an AU. The straight-forward approach is to use multiple cameras with different camera parameter settings to record the same input scene. However, this approach is impractical as there are thousands of different combinations of even just the four camera parameters we consider. To overcome the challenge, we proceed with two workarounds.

**Experiment 1: working with a real-camera.** To see the impact of camera settings on a real camera, we simulate DAY and NIGHT conditions in our lab and evaluate the performance of the most accurate face-recognition AU (Neoface-v3 (Patrick Grother & Hanaoka, 2019)<sup>1</sup>. We use two sources of light and keep one of them always ON, while the other light is manually turned ON or OFF to emulate DAY and NIGHT conditions, respectively.

We place face cutouts of 10 unique individuals in front of the camera and run the face recognition pipeline for various camera settings and for different face matching thresholds.

<sup>1</sup>This face-recognition AU is ranked first in the world in the most recent face-recognition technology benchmarking by NIST.

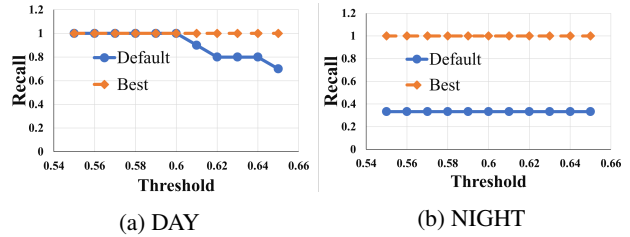


Figure 3. Parameter tuning impact for Face-recognition AU.

Since this face-recognition AU has high precision despite environment changes, we focus on measuring Recall, *i.e.*, true-positive rate. We compare AU results under the “Default” camera settings, *i.e.*, the default values provided by the manufacturer, and “Best” settings for the four camera parameters. To find the “Best” settings, we change the four camera parameters using the VAPIX API (Communications) provided by the camera vendor to find the setting that gives the highest Recall value. Specifically, we vary each parameter from 0 to 100 in steps of 10 and capture the frame for each camera setting. This gives us  $\approx 14.6K$  ( $11^4$ ) frames for each condition. Changing one camera setting through the VAPIX API takes about 200ms, and in total it took about 7 hours to capture and process the frames for each condition.

Figure 3a shows the Recall for the DAY condition for various thresholds and Figure 3b shows the Recall for the NIGHT condition for various thresholds. We see that under the “Default” settings, the Recall for the DAY condition goes down at higher thresholds, indicating that some faces were not recognized, whereas for the NIGHT condition, the Recall remains constant at a low value for all thresholds, indicating that some faces were not being recognized regardless of the face matching thresholds. In contrast, when we changed the camera parameters for both conditions to the “Best” settings, the AU achieves the highest Recall (100%), confirming that all the faces are correctly recognized. These results show that it is indeed possible to improve AU accuracy by adjusting the four camera parameters.

**Experiment 2: working with pre-recorded videos.** The pre-recorded videos from public datasets are already captured with certain camera parameter settings, and hence we do not have the opportunity to change the real camera parameters and observe their impact. As an approximation, we apply different values of brightness, contrast, color-saturation and sharpness to these pre-recorded videos using several image transformation algorithms in the Python Imaging Library (PIL) (Clark & Contributors), and then observe the impact of such transformation on accuracy of AU insights.

We consider 19 video snippets from the HMDB dataset (Kuehne et al., 2011) and 11 video snippets from the Olympics dataset (Niebles et al., 2010). Using cvat-tool (opencv-toolkit), we manually annotated the face and person bounding boxes to form our ground truth. Each

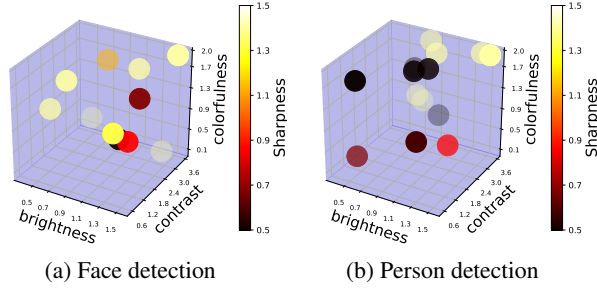


Figure 4. Distribution of best transformation tuple for two AUs on HMDB video snippets.

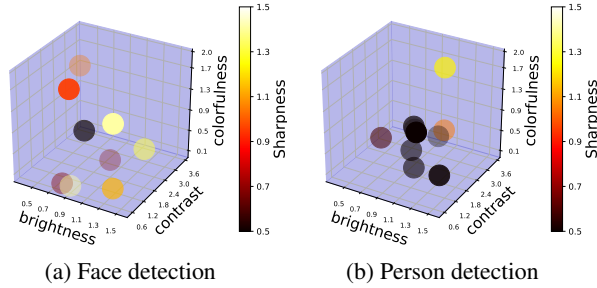


Figure 5. Distribution of best transformation tuple for two AUs on Olympics video snippets.

video-snippet contains no more than a few hundred frames, and the environmental conditions vary across the video snippets due to change in video capture locations. We determine a single best tuple of those four transformations for each video, *i.e.*, one that results in the highest analytical quality for that video. Figure 4 and Figure 5 show the distribution of the best transformation tuples for the videos in the two datasets, respectively. We see that with a few exceptions, the best transformation tuples for different videos in a dataset do not cluster, suggesting that any fixed real camera parameter settings will not be ideal for different environmental conditions or analytics tasks. Table 1 shows the maximum and average analytical quality improvement achieved after transforming each video-snippet as per their best transformation tuple. We observe up to 58% improvement in accuracy of insights when appropriate transformations or equivalent camera parameters are applied.

Finally, we applied the above process of searching for the best camera settings to 1-per-second sampled frames in the day-long video in §3.1. The green bars in Figure 2a and Figure 2b show that for face detection, the average mAP values for the optimal settings are 6.1% – 15.7% higher than for the default settings, and for person detection the average mAP values under optimal settings are 4.9% – 9.7% higher than under the default settings. These results suggest that the impact of environment on the accuracy of AUs can be remedied by tuning the four camera parameters to improve the image capture process.

Table 1. Accuracy improvement of best configuration .

Video-Dataset	AU	mAP improvement	
		Max	Mean
		Olympics	Face Detection
	Person Detection	40.38	8.38
HMDB	Face Detection	18.75	4.22
	Person Detection	57.59	12.63

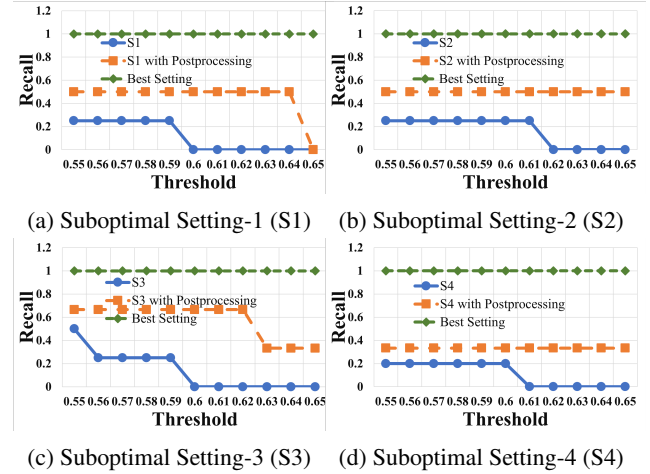


Figure 6. Parameter tuning vs. postprocessing for NIGHT.

### 3.3 Post-capture Image Processing is Not Enough

It is important to note that modifying camera parameters to capture a better image or video feed is fundamentally different from applying transformations to the frames already retrieved from the camera. In particular, if the image captured by the camera is sufficiently poor due to sub-optimal camera settings, no further transformations of the video stream from the camera can improve the accuracy of analytics. To see this, we repeated the same face-recognition AU experiment with a real camera in §3.2, by intentionally changing the default camera parameters to specific sub-optimal settings denoted by S1, S2, S3 and S4 and measured the Recall for face recognition AU as before. In these settings, the frames from the camera are of poor quality and the Recall for various thresholds are quite low for all settings. Then, we apply digital transformation on these and note the highest Recall value that we can obtain.

Figure 6 shows the results for parameter tuning and post-capture transformations. We see that for each of the four sub-optimal camera settings, post-processing improved the Recall compared to the original video, but the Recall is still quite low. In contrast, if we directly change the actual camera parameters, shown as “Best setting”, then we are able to achieve the highest possible Recall (*i.e.*, 100%).

## 4 CHALLENGES AND APPROACHES

We faced several challenges while designing CAMTUNER. In this section, we discuss these challenges and our approaches to address each one of them.



**Challenge 1: Identifying best camera settings for a particular scene.** Cameras deployed across different locations observe different scenes. Moreover, the scene observed by a particular camera at any one location keeps changing based on the environmental conditions, lighting conditions, movement of objects in the field of view, etc. In such a dynamic environment, how can we identify the best camera settings that will give the highest AU accuracy for a particular scene? The straight-forward approach to collect data for all possible scenes that can ever be observed by the camera and train a model that gives the best camera settings for a given scene is infeasible.

**Approach.** To address this challenge, we propose to use an online learning method. Particularly, we use Reinforcement Learning (RL) (Sutton et al., 1998), in which the agent learns the best camera settings on-the-go. Out of several recent RL algorithms, we choose the SARSA (Wiering & Schmidhuber, 1998) RL algorithm for identifying the best camera settings (more details provided in §5.1).

**Challenge 2: No Ground truth in real time.** Implementing online RL requires knowing the reward/penalty for every action taken during exploration and during exploitation, *i.e.*, what effect will a particular camera parameter setting have on the accuracy change of the AU. Since no ground truth of the AU task, *e.g.*, face detection, is available during normal operation of the real time video analytics system, detecting a change in accuracy of the AU during runtime is challenging.

**Approach.** We propose to *estimate* the accuracy of the AU. Each AU, depending on its function, has a preferred method of measuring accuracy, *e.g.*, for a face detection AU, a combination of mAP and true-positive IoU is used, whereas for a face recognition AU, true-positive match score is used. Accordingly, we propose to have a separate estimator for each AU. We design such *AU-specific analytics quality estimators* to be light-weight so that they can be used by the RL agent in real time (more details provided in §5.2).

**Challenge 3: Extremely slow initial RL training.** Online learning at each camera deployment setup requires initial RL training, which can potentially take a very long time for two key reasons: (1) Capturing the environmental condition changes such as the time-of-the-day effect requires waiting for the Sun’s movement through the entire day until night, and capturing weather changes requires waiting for weather changes to actually happen. (2) Taking an action on the real camera, *i.e.*, changing camera parameter settings, incurs a significant delay of about 200 ms. This delay fundamentally limits the speed of state transition and hence the learning speed of RL to only 5 actions per second.

**Approach.** In order to speed up the initial RL training, we propose a novel concept called *Virtual Camera (VC)*. A VC mimics the effect of environmental conditions and camera

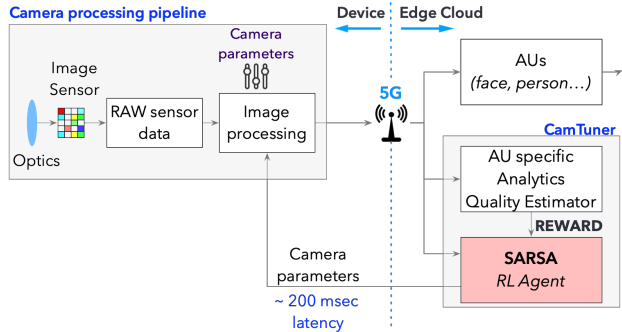


Figure 7. CamTuner system design.

settings change on the frame capture of a real camera. This has two immediate benefits. First, it can effectively complete an action of “camera setting change” almost instantaneously. Second, it can augment a single frame captured by the real camera with many new transformed frames as if they were captured by the real camera under different conditions. Together, these two benefits allow the RL system to explore an order of magnitude more states and actions per unit time (more details provided in §5.3).

## 5 CamTuner DESIGN

Figure 7 shows the system-level architecture for CAMTUNER, which automatically and dynamically tunes the camera parameters to optimize the accuracy of AUs in the VAP. CAMTUNER augments a standard VAP shown in Figure 1 with two key components: a Reinforcement Learning (RL) engine, and an AU-specific analytics quality estimator. In addition, it employs a third component, a Virtual Camera (VC), for fast initial RL training.

### 5.1 Reinforcement Learning (RL) Engine

The RL engine is the heart of CAMTUNER system, as it is the one that automatically chooses the best camera settings for a particular scene. Q-learning (Watkins & Dayan, 1992) and SARSA (Wiering & Schmidhuber, 1998) are two popular RL algorithms that are quite effective in learning the best action to take in order to maximize the reward. We compared these two algorithms and found that training with SARSA achieves slightly faster convergence and also slightly better accuracy than with Q-learning. Therefore, we use SARSA RL algorithm in CAMTUNER.

SARSA is similar to other RL algorithms. An agent interacts with the environment (*state*) it is in, by taking different *actions*. As the agent takes actions, it moves into a new state or environment. For each action, there is an associated *reward* or penalty, depending on whether the new state is desirable or not. Over a period of time, as the agent continues taking actions and receiving rewards and penalties, it learns to maximize the rewards by taking the right actions, which ultimately lead the agent towards desirable states.

SARSA does not require any labeled data or pre-trained

model, but it does require a clear definition of the *state*, *action* and *reward* for the RL agent. This combination of *state*, *action* and *reward* is unique for each application and needs to be carefully chosen, so that the agent learns exactly what is desired. In our setup, we define them as follows:

**State:** A state is a tuple of two vectors,  $s = \langle P_t, M_t \rangle$ , where  $P_t$  consists of the current brightness, contrast, sharpness and color parameter values on the camera, and  $M_t$  consists of the brightness, contrast, sharpness and color-saturation values of the captured frame at time  $t$ .

**Action:** The set of actions that the agent can take are (a) increase or decrease one of the brightness, contrast, sharpness or color-saturation parameter value, or (b) not change any parameter values.

**Reward:** We use an AU-specific analytics quality estimator as the reward function for the SARSA algorithm.

## 5.2 AU-specific Analytics Quality Estimator

In online operations, the RL engine needs to know whether its actions are changing the AU accuracy in the positive or negative direction. In the absence of ground truth, the *analytics quality estimator* acts as a guide and generates the reward/penalty for the RL agent.

**Challenges.** There are three key challenges in designing an online analytics quality estimator. (1) During runtime, AU quality estimation has to be done quickly, which implies a model that is small in size. (2) A small model size implies using a shallow neural network. For such a network, what representative features should the estimator extract that will have the most impact on the accuracy of AU output? (3) Since different types of AUs (*e.g.*, face detector, person detector) perceive the same representative features differently, the estimator needs to be AU-specific.

**Insights.** We make the following observations about estimating the quality of AUs. (1) Though estimating the precise accuracy of AU on a frame requires a deep neural network, estimating the coarse-grained accuracy, *e.g.*, in increments of 1%, may only require a shallow neural network. (2) Most of the “off-the-shelf” AUs use convolution and pooling layers to extract representative local features (Chen et al., 2019). In particular, the first few layers in the AUs extract low-level features such as edges, shapes, or stretched patterns that affect the accuracy of the AU results. We can reuse the first few layers of these AUs in our estimator to capture the low-level features. (3) To capture different AU perceptions from the same representative features extracted in the early layers, we need to design and train the last few layers of each quality estimator to be AU-specific. During training, we need to use AU-specific quality labels.

**Design.** Motivated by the above insights, we design our lightweight AU-specific analytical quality estimator that

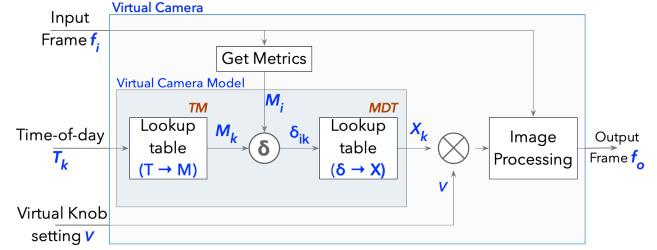


Figure 8. VC block diagram.

has two components: (1) feature extractor and (2) quality classifier, as shown in Figure 11. We use supervised learning to train the AU-specific quality estimator.

**Feature Extractor.** Different AUs and environmental conditions can manipulate local features of an input frame at different granularities (Gupta et al., 2021). For example, blur (*i.e.*, motion or defocus blur) affects fine textures while light exposure affects coarse textures. While face detector and face recognition AUs focus on finer face details, person detector is coarse-grained and it only detects the bounding box of a person. Similarly, in convolution layers, larger filter sizes focus on global features while stacked convolution layers extract fine-grained features. To accommodate such diverse notions of granularities, we use the Inception module from the Inception-v3 network (Szegedy et al., 2016), which has convolution layers with diverse filter sizes.

**Quality classifier.** The goal of the quality classifier is to take the features extracted by the feature extractor and estimate the coarse-grained accuracy of the AU on an input frame, *e.g.*, in increments of 1%. As such, we divide the AU-specific accuracy measure into multiple coarse-grained labels, *e.g.*, from 0% to 99%, and use fully-connected layers whose output nodes generate AU-specific classification labels.

Detailed design and training of two concrete AU-specific analytics quality estimators can be found in Appendix A2.

## 5.3 Virtual Camera

**Definition.** A VC (shown in Figure 8) takes an input frame  $f_i$ , captured by a real camera, the target time-of-the-day  $T_k$ , and VC parameter settings  $V$ , as input, and outputs a frame  $f_o$  as if it was captured by the physical camera at time  $T_k$ . To generate a frame at time  $T_k$ , VC uses a composition function  $Compose(X_k, V)$ , which composes output frame  $f_o$  using  $X_k$ , which is the transformation that augments the environmental effects corresponding to the target time  $T_k$  on input frame  $f_i$ , and  $V$ , which is the VC parameter settings. The composition function is defined as  $X_k * 10^{V-0.5}$ , which considers  $X_k$  and  $V$  simultaneously, similar to a real camera. Using this composition function,  $X_k$  is scaled up if the value of  $V$  is greater than 0.5 and scaled down if the value is less than 0.5; no scaling of  $X_k$  happens for  $V$  equal to 0.5.

To understand how VC works, we first introduce an impor-

tant definition. Each frame  $f_i$ , from a real physical camera, possesses distinct values of brightness, contrast, colorfulness and sharpness metrics, denoted as a *metric (or feature) tuple*  $M_i = \langle \alpha_M, \beta_M, \gamma_M, \zeta_M \rangle$ . The unique metric tuple encapsulates the environmental conditions and the default physical camera settings when the frame was captured.

A VC derives two tables for a given physical camera deployment during an offline profiling phase (details can be found in Appendix A3) and then uses the two tables during online operation to generate the output frame  $f_o$ .

**Online phase.** VC transforms the input frame  $f_i$  to output frame  $f_o$  in five steps. (1) It measures the current metric tuple  $M_i = \langle \alpha_M, \beta_M, \gamma_M, \zeta_M \rangle_{curr}$  from input frame  $f_i$ ; (2) It looks up a *Time-to-Metric (TM)* table for the metric tuple  $M_k = \langle \alpha_M, \beta_M, \gamma_M, \zeta_M \rangle_{desired}$  that corresponds to the target time of the day ( $T_k$ ); (3) It calculates the difference between  $M_i$  and  $M_k$ ,  $\delta(M_i, M_k)$  or  $\delta_{ik}$ ; (4) It looks up a *Metric-difference-to-Transformation (MDT)* table to find the transformation  $X_k = \langle \alpha_X, \beta_X, \gamma_X, \zeta_X \rangle_{applied}$  that corresponds to  $\delta_{ik}$ ; (5) It applies  $X_k$  along with  $V$  using the composition function  $Compose(X_k, V)$  to input frame  $f_i$  and generates output frame  $f_o$ .

Since different parts of an input frame may exhibit varying local feature or metric values, to improve the effectiveness of virtual knob transformation, instead of applying the above steps directly to input frame  $f_i$ , we split it into 12 (3 X 4) equal-sized tiles, apply Steps 1-3 to each of the 12 tiles, *i.e.*, each of  $M_i$ ,  $M_k$ , and  $\delta_{ik}$  consists of 12 sub-tuples corresponding to the 12 tiles, respectively. The 12 sub-tuples in  $\delta_{ik}$  are looked up in the MDT table to find 12 transformation tuples. Finally, to ensure smoothness, we calculate the mean of these 12 sub-tuples  $X_k$ , which is then applied to input frame  $f_i$ .

#### 5.4 Integrating VC with the RL engine

During initial RL training, the RL agent performs fast exploration by leveraging VC as follows. It reads each frame  $f_i$  from the input training video, and repeats the following exploration steps for all time-of-the-day values  $T_k$ . At each exploration step  $j$ , the agent which is at state  $s = \langle P_j, M_j \rangle$  performs tasks: (1) based on current state ( $s$ ), it takes a random action  $a$  and apply that on  $V_j$ , which is VC equivalent of  $P_j$  for a real camera, to get a new virtual knob setting for next exploration step ( $j + 1$ ),  $V_{j+1}$ ; (2) it invokes the VC with frame  $f_i$  for the target time-of-the-day  $T_k$ , and current VC parameters  $V_{j+1}$  as input, and the VC outputs frame  $f_o$ . The measured tuple  $M_{j+1}$  of brightness, contrast, colorfulness and sharpness metric values of output frame  $f_o$  along with the virtual knob setting  $V_{j+1}$ , form the new state of the RL agent,  $s_{new} = \langle V_{j+1}, M_{j+1} \rangle$ ; (3) it calculates the reward/penalty by feeding  $f_o$  into the AU-specific quality estimator; and (4) it updates the Q-table entry  $Q(s, a)$ .

Table 2. Accuracy of VC.

Parameter	Brightness	Contrast -Saturation	Color	Sharpness
Mean error	5.4 %	13.8 %	17.3 %	19.8 %
Std. dev.	1.7 %	4.3 %	9.6 %	8.1 %

The above initially trained SARSA model with the VC is then deployed in the real camera for the normal operations of CAMTUNER. First, the  $\epsilon$  value is set to low (0.1) so that the SARSA RL agent will go through an *adaptation* phase, *e.g.*, for an hour, by performing primarily exploration. Afterwards, the  $\epsilon$  value is set to high (0.9) so that SARSA performs primarily exploitation using the trained model.

## 6 EVALUATION

We extensively evaluate the effectiveness of CAMTUNER by evaluating the efficacy of its components, its impact on AU accuracy improvement in a VAP via emulation and in a real deployment, as well as its system overhead.

### 6.1 Offline Model Training

We first evaluate the efficacy of two key components of CAMTUNER which are trained offline: VC and AU-specific analytics quality estimator model.

**Virtual camera.** VC is designed to render a frame taken at one time ( $T_1$ ) to any other time ( $T_2$ ), as if the rendered frame were captured at time  $T_2$ . First, we trained the VC following Appendix A3 using a 24-hour long video obtained from one of our customer locations at an airport. To evaluate how well VC works online, we obtain several video snippets at 6 different hours of the day from the same camera. Next, we feed 1 video snippet  $VS_0$  from one particular hour  $H_0$  through the VC to generate 5 video snippets  $VS_j$  corresponding to the hours of the other 5 videos. For each generated video snippet  $VS_j$ , we calculate the relative error of the metric tuple values of each frame in  $VS_j$  relative to that of the corresponding original video frame and average such error across all the frames in  $VS_j$  (over 37.5K frames). We obtain 5 VC error metric tuples for one video, each corresponding to the hour of the other 5 video snippets. We repeat the above experiment for the 5 other original video snippets to obtain a total of 30 VC error tuples. Table 2 shows the mean error and standard deviation among all 30 VC error tuples. We observe that the average VC errors are 5.4%, 13.8%, 17.3%, and 9.8% for brightness, contrast, color-saturation and sharpness, respectively.

**AU-specific analytics quality estimator.** Next, we evaluate the performance of AU-specific quality estimators by measuring the Spearman and Pearson correlation between quality estimates by the estimators and the analytical quality derived using ground truth, for three different AUs. First, we trained the face-recognition, face-detection, and person-detection estimators through supervised learning as described in Appendix A2. To evaluate the face-recognition estimator, we used the celebA-validation dataset which con-



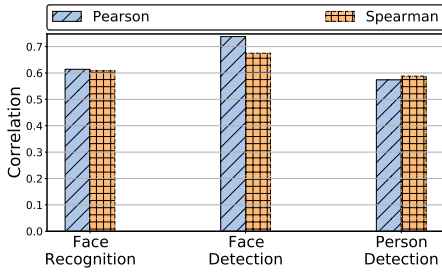


Figure 9. AU-specific analytics quality estimator Performance

tains 200 images (*i.e.*, different from the 300 original training images used in Appendix A2) and their about 2 million variants from augmenting the original images using the python-pil image library (Clark & Contributors). Figure 9 shows the quality predicted by the face-recognition analytics quality estimator is strongly correlated with the output by the AU (both Pearson and Spearman correlation are greater than 0.6) (Statisticssolutions, 2019; BMJ, 2019).

To evaluate face-detection and person-detection estimators, we used annotated video frames from the *olympics* (Niebles et al., 2010) and *HMDB* datasets (Kuehne et al., 2011) and their 4 million variants that were generated. Figure 9 shows there is a strong positive correlation between the measured mAP and IoU metric and the predicted quality estimate for both face-detection and person-detection AUs. In summary, the strong correlation between the prediction by the estimators and the actual quality of AUs based on ground truth enables CAMTUNER’s RL agent to effectively tune camera parameters.

## 6.2 End-to-end VAP Accuracy (Ablation Study)

**Hardware setup.** For this study, we use an *AXIS Q6128-E* network surveillance camera. We ran CAMTUNER on a low-end *Intel NUC box* while the face detection and person detection AUs and initial pre-training with VC run on a high-end edge-server equipped with Xeon(R) W-2145 CPU and GeForce RTX 2080 GPU. The captured frames are sent for AU processing to the edge-server over a 5G network with an average offload latency of 39.7 ms.

**Baseline VAPs and CAMTUNER variants.** We compare our CAMTUNER against two different baseline VAPs. (1) *Baseline*: In the Baseline VAP, the camera parameters are not adapted to any changes. (2) *Strawman*: The Strawman approach applies a time-of-the-day heuristic and tunes the four camera parameters based on human perception. In particular, we use the BRISQUE quality metric and exhaustively search for the best camera parameters for the first few frames in each hour and then apply those best camera settings for the remaining frames in that hour. This exhaustive search for initial frames takes a few minutes and our results show that doing this periodic adaptation does not give significant improvement.

We evaluate two variants of CAMTUNER. (3) CAMTUNER-

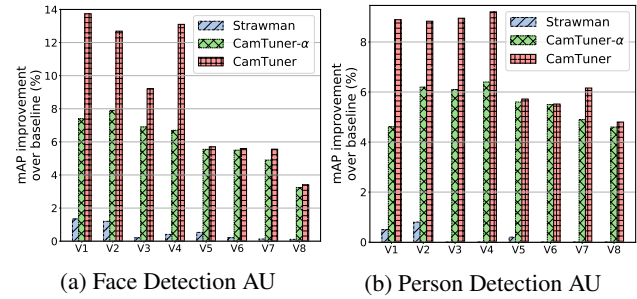


Figure 10. mAP improvements for different AUs.

$\alpha$ : This variant of CAMTUNER adjusts camera settings dynamically by using only the offline trained SARSA RL agent, *i.e.*, the agent does not perform any exploration during online operation. (4) CAMTUNER: Final CAMTUNER framework, which is seeded with offline trained SARSA RL agent, and then during online operation, the agent continues exploration initially and then moves towards exploitation, as described in §5.4. For CAMTUNER- $\alpha$  and CAMTUNER, the RL agent adaptively adjusts the four camera parameters periodically (the time interval is configurable and we choose it to be 1 minute).

**Experimental methodology.** We loop a pre-recorded (original) 5-minute video snippet (a customer video captured at an airport) through four different VCs – these VCs are not for RL training but serve as inputs to the four VAPs. For the VCs, we gradually change the VC model parameters (*i.e.*, transformations) to simulate the changes that happen during the day as the Sun changes its position and finally sets.

VAP 1 does not adjust camera settings, while VAP 2, VAP 3, and VAP 4 use Strawman, CAMTUNER- $\alpha$ , and CAMTUNER, respectively, to adaptively adjust camera settings.

**Results.** We evaluate the AU accuracy improvement of VAPs 2-4 over VAP 1 for 8 randomly selected 5-minute time segments throughout the day (the time-segments are separated by at least 1 hour), with each segment consisting of 7500 frames. The ground-truth analytics results are obtained for the video segments via cvat-tool to evaluate the detection accuracy (mAP) of the 4 VAPs.

Figure 10 shows the bar-plot of mAP improvement of VAPs 2-4 over VAP 1 for the eight 5-min video segments. We make the following observations. The strawman approach based on *time-of-the-day* heuristic can provide only nominal improvement than Baseline, *i.e.*, on average less than 1% for both face detection and person detection. In contrast, dynamically adjusting the four virtual knobs using CAMTUNER- $\alpha$  improves face detection accuracy by 6.01% on average and person detection accuracy by 5.49% on average over the baseline approach. Finally, dynamically tuning the real camera parameters with online learning in CAMTUNER improves the face detection AU accuracy up to 13.8% and person detection AU accuracy up to 9.2%. Also, we observe an average improvement of 8.63% and 8.11% for face de-

tection AU, and average improvement of 7.25% and 7.08% for person detection AU compared to static and strawman approach, respectively.

### 6.3 Experiences in Real-world Deployment

To validate that similar accuracy improvement from video-playback in §6.2 is achieved in real-world deployment where the parameters of the camera are continuously re-configured, we evaluated our deployment of CAMTUNER at one of our customer deployment sites. The VAP deployment uses an AXIS Q6128-E PTZ network camera-1 that uploads the captured frames over 5G network to a remote high-end PC server (with a Xeon processor and NVIDIA GPU) running face detection AU (VAP 1). The captured frames are also sent in parallel to CAMTUNER which runs on low-end Intel-NUC box (with a 2.6 GHz Intel i7-6770HQ CPU), seeded with the initially VC-trained RL agent as in §6.2.

To evaluate the accuracy of the VAP, we deployed a second, temporary VAP using a second, identical camera, camera-2, deployed side-by-side with the original camera-1, and running its own AU, and ensured that both cameras view almost identical scene at the same time. The captured frames from camera-2 are sent to the face detection AU (VAP 2).

We ran both VAPs side-by-side for 6 continuous hours in a day. During the experiment, we recorded all captured frames and their respective predictions from both VAPs. We annotated the recorded frames with ground-truth using cvat-tool and measured the mAP of face detection by both VAPs. The mAP for the VAP with camera-1 (79.5%) is 11.7% higher than that of the VAP with camera-2 (67.8%).

### 6.4 System Overhead

Since CAMTUNER system runs in parallel with the AU, it does not add any additional latency to the video analytic pipeline and hence the AU latency. In the following, we show that the normal online operation of CAMTUNER is light-weight, and the initial training phase using the VC can explore each action fast.

First, in online operations, each iteration of CAMTUNER involves three tasks: evaluating the AU-specific quality estimator, evaluating the Q-function by the SARSA agent, and changing the parameters of the physical camera. We run CAMTUNER on a low-end edge device, an Intel-NUC box equipped with a 2.6 GHz Intel i7-6770HQ CPU. The AU-specific quality estimator takes 40ms and the SARSA RL agent takes less than 1ms to complete Q-function calculation and Q-table update. Since the two tasks can be pipelined with changing the physical camera settings which takes 200ms on the AXIS Q6128-E Network camera we used, each iteration of CAMTUNER takes 200ms, *i.e.*, 5 iterations per second, and the average CPU utilization is only 15% with 150 MB memory footprint.

Next, we run the initial RL training phase on a high-end PC with a 3.70 GHz Intel(R) Xeon(R) W-2145 CPU and

GeForce RTX 2080 GPU. During the one-hour training phase performed in §6.1, in each iteration of the RL exploration, the VC takes 4 ms to output  $f_o$ , the quality estimator takes 10 ms, and the RL agent take less than 1 ms to evaluate the Q-function and update the Q-table, for a total of 15 ms. As a result the CAMTUNER can explore around 70 actions per second, which is 14X faster than using the physical camera. The CPU utilization is steady at 60%.

## 7 RELATED WORK

To our best knowledge, CAMTUNER is the first system that adaptively learns the best settings for a camera deployed in the field as part of a VAP in reaction to environmental condition changes to improve the AU accuracy.

Several work investigated tuning parameters of VAP after camera capture and before sending it to AU or changing the AU based on the input video content. Videostorm (Zhang et al., 2017), Chameleon (Jiang et al., 2018), and Awestream (Zhang et al., 2018) tune the after-capture video stream parameters like frames-per-second or frame resolution to ensure efficient resource usage while processing video analytics queries at scale. As discussed in §3.3, processing images after capture cannot correct image quality well, if the camera was operating under sub-optimal settings.

More recent work, *e.g.*, Focus (Hsieh et al., 2018), NoScope (Kang et al., 2017), Ekya (Padmanabhan et al.), and AMS (Khani et al., 2020), studied how to adapt AU model parameters based on captured video content. Such an approach requires additional GPU resources for periodic re-training and is also less reactive to the video content changes. In contrast, CAMTUNER adapts the camera parameters in real time according to environment changes.

Several frame filtering techniques on edge devices (Canel et al., 2019; Paul et al., 2021; Chen et al., 2015; Li et al., 2020) can work in conjunction with CAMTUNER and potentially further improve CAMTUNER’s performance. Our AU-specific analytics quality estimator shares similar goal as the AQuA-quality estimator (Paul et al., 2021) but differs in that CAMTUNER’s quality estimator performs fine-grained quality estimation that is specific to each AU, while AQuA performs coarse-grained AU-agnostic image quality estimation.

There is a large body of work on configuring the image signal processing pipeline (ISP) in cameras to improve human-perceived quality of images from the cameras, *e.g.*, (Wu et al., 2019; Liu et al., 2020; Diamond et al., 2021; Nishimura et al., 2019). In contrast, we study dynamic camera parameter tuning to optimize the accuracy of VAPs.

## 8 CONCLUSION

In this paper, we showed that in a typical surveillance camera deployment, environmental condition changes can significantly affect the accuracy of analytics units in a VAP. We developed CAMTUNER, a system that dynamically adapts complex settings of the camera in a VAP to changing envi-

ronmental conditions to improve the AU accuracy. Through dynamic tuning, CAMTUNER is able to achieve up to 13.8% and 9.2% higher accuracy for the face detection AU and person detection AU respectively, compared to the best of the two approaches i.e., baseline and strawman approach (average improvement of  $\sim 8\%$  for both face detection AU and person detection AU). The CAMTUNER-enhanced VAP has been running at our customer sites since Summer 2021, and shown to improve the accuracy of the face detection AU by 11.7% compared to the original VAP without CAMTUNER. We believe CAMTUNER’s system design and key components, Virtual camera and light-weight AU-specific analytics quality estimators, can be applied to dynamically tune other complex sensors such as depth and thermal cameras.

## APPENDIX

### A1. Parameters exposed by popular cameras

Table 3 in Appendix lists the parameters exposed by a few popular cameras in the market today.

Table 3. Parameters exposed by popular cameras.

Camera Settings	Image Appearance	Brightness sharpness contrast color level
	Exposure Settings	Exposure Value Exposure Control Max Exposure Time Exposure Zones Max Shutter Max gain IR cut filter
	Image Settings	Defog Effect Noise Reduction Stabilizer Auto Focus Enabled
	White Balance	Type window
Video Stream	Image Appearance	Resolution Compression Rotate image
	Encoder Settings	GOP length H.264 profile
	Bitrate Control	Type of Use Target Bitrate Priority
	Video Stream	Max Frame rate

### A2. Case Studies of AU-specific Analytics Quality Estimator Design

Here, we describe the AU-specific quality classifier design and training for two specific AUs.

(1) *Face recognition AU*: The quality classifier of face recognition consists of 2 fully-connected layer and has 101 output classes. One of the classes signifies no match, while the remaining 100 classes correspond to match scores between 0 to 100% in units of 1%.

To generate the labeled data, we used 300 randomly-sampled celebrities from the celebA dataset (Liu et al., 2015). We choose two images per person. We use one of them as a reference image and add it to the gallery. We use the other image to generate multiple variants by changing the virtual knob values. These variants ( $\sim 4$  million) form the query images. For each query image, we obtain the match score (a value between 0 and 100%) using the Face recognition AU, *Neoface-v3*. The query images along with their match score form the labeled samples, which are used to train the quality estimator.

(2) *Person and face detection AU*. The quality classifier of

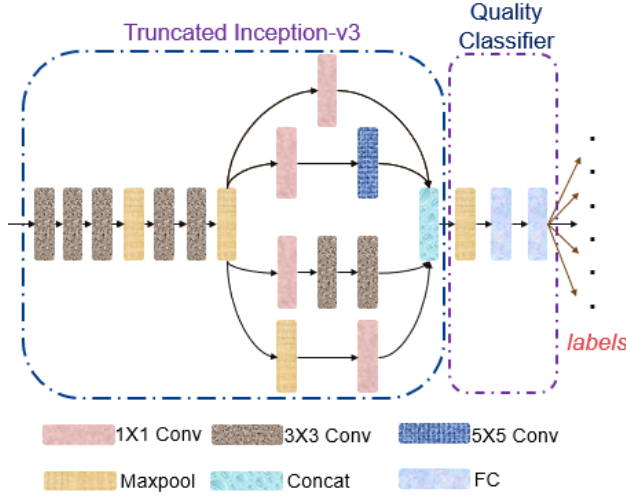


Figure 11. AU-specific analytics quality estimator design.

person and face detection AU consists of 2 fully-connected layers, and has 201 output classes to predict the quality estimate of the person and face detection AU for a given frame. One of the classes signifies AU cannot detect anything accurately, and the remaining 200 classes correspond to the cumulative mAP score between 0 to 100 and IoU score between 0 to 100, *i.e.*,  $mAP + IOU_{True-Positive} * 100$ . To generate the labeled data, we used the Olympics (Niebles et al., 2010) and HMDB (Kuehne et al., 2011) datasets, and created  $\sim 7.5$  million variants of the video frames by changing virtual knob values. Then, for each frame, we use the detection AU to determine the analytical quality estimate. The video frames and their quality estimates form the labeled samples, which are used to train the estimator model.

For both the classifier training, we use a cross-entropy loss function to train AU-specific analytics quality estimators, initial learning rate is  $10^{-5}$ , and we use Adam Optimizer (Kingma & Ba, 2014)

### A3. Offline Table Constructions in VC

**Offline profiling phase:** In this phase, we construct the two mapping tables.

The first table (TM) maps a given time-of-the-day  $T_k$  to the metric tuple  $M_k$  which captures the distinct values of brightness, contrast, colorfulness and sharpness metrics of frames taken by the physical camera with the default settings at time  $T_k$ . We generate the table to cover the full 24-hour period with a granularity of 15 minutes, *i.e.*, the table has one mapping for every 15 minutes, for a total of 96 mappings. To construct the table, we use a full 24-hour long video and break it into 15-minute video snippets. We extract all the frames from the video snippet for each 15-minute interval  $T_k$ . We divide each frame into 12 tiles, obtain the

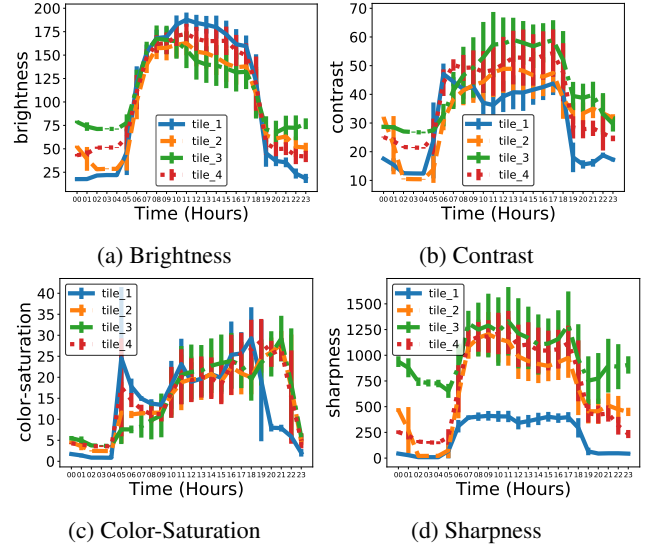


Figure 12. Day-long feature profiles for different tiles

corresponding metric tuple for each tile, and compute the mean metric tuple for the corresponding tiles in all frames in the 15-minute interval as the metric tuple for that tile, and the list of tuples for all 12 tiles form the entry for time  $T_k$  in the table, as shown in Figure 13a.

The second table (MDT) maps the difference between two metric tuples  $M_i$  and  $M_k$ ,  $\delta(M_i, M_k)$ , to the corresponding transformation tuple  $X_k$  that would effectively transform a frame captured by the physical camera with metric tuple  $M_k$  to become a frame captured by the physical camera for the same scene with metric tuple  $M_i$ . We note since each camera setting can take 11 values, from 0 to 100 with increments of 10, the total number of possible difference between any two metric tuples is 14K ( $11^4$ ). We construct the entries for the table backwards as follows. (1) We select a random frame from each 15-minute interval to form a collection of 96 frames with varying environmental conditions, *i.e.*, corresponding to different time-of-the-day. (2) For each possible transformation  $X_k$ , we transform the 96 frames into 96 virtual frames. We then obtain the delta metric tuples between each pair of original and transformed frames, calculate the median of the 96 delta metric tuples,  $\delta_k$ , and store the pair of  $\langle \delta_k, X_k \rangle$  in the table. (3) We repeat above the process for all possible possible transformation settings (14K in total) to populate the table, as shown in Figure 13b. Finally, at runtime when the table is used by the VC, if the entry for a given delta metric tuple  $\delta_i$  is empty, we return the entry whose delta metric tuple  $\delta_k$  is closest to  $\delta_i$  using L1-norm.

Time-of-day ( $T_i$ )	Metric Tuple ( $M_i$ )			Delta Change ( $\delta$ )	Transformation Tuple ( $X$ )
	tile_1	tile_2	.....		
10:00	<159,53,1,1,2122>	<157,55,9,2103>	.....	<0.5,0.7,1.5,2>	<0.7,0.6,1.1,1.2>
10:15	<160,52,1,3,2100>	<159,56,1,5,2080>	.....	<10,18,5,9>	<1.5,2.4,1.6,1.5>
.....	.....	.....	.....	.....	.....

(a) TM table

(b) MDT Table

Figure 13. Offline generated tables.

## REFERENCES

- Vp9. <https://www.webmproject.org/vp9/>, 2017.
- x264. <http://www.videolan.org/developers/x264.html>, 2021.
- Bayer, B. E. Color imaging array, July 20 1976. US Patent 3,971,065.
- BMJ, T. correlation-and-regression. <https://www.bmj.com/about-bmj/resources-readers/publications/statistics-square-one/11-correlation-and-regression>, 2019.
- Canel, C., Kim, T., Zhou, G., Li, C., Lim, H., Andersen, D. G., Kaminsky, M., and Dulloor, S. Scaling video analytics on constrained edge nodes. In Talwalkar, A., Smith, V., and Zaharia, M. (eds.), *Proceedings of Machine Learning and Systems*, volume 1, pp. 406–417, 2019. URL <https://proceedings.mlsys.org/paper/2019/file/85d8ce590ad8981ca2c8286f79f59954-Paper.pdf>.
- Chen, E. H., Röthig, P., Zeisler, J., and Burschka, D. Investigating low level features in cnn for traffic sign detection and recognition. In *2019 IEEE Intelligent Transportation Systems Conference (ITSC)*, pp. 325–332, 2019. doi: 10.1109/ITSC.2019.8917340.
- Chen, T. Y.-H., Ravindranath, L., Deng, S., Bahl, P., and Balakrishnan, H. Glimpse: Continuous, real-time object recognition on mobile devices. In *Proceedings of the 13th ACM Conference on Embedded Networked Sensor Systems*, pp. 155–168, 2015.
- CISCO. Cisco video surveillance ip cameras. <https://www.cisco.com/c/en/us/products/physical-security/video-surveillance-ip-cameras/index.html>.
- Clark, A. and Contributors. Pillow library. <https://pillow.readthedocs.io/en/stable/>.
- CNET. How 5g aims to end network latency. CNET\_5G\_network\_latency\_time, 2019.
- cocoapi github. pycocotools. <https://github.com/cocodataset/cocoapi/tree/master/PythonAPI/pycocotools>.
- Communication, A. Axis network cameras. <https://www.axis.com/products/network-cameras>.
- Communications, A. Vapix library. URL <https://www.axis.com/vapix-library/>.
- Deng, J., Guo, J., Yuxiang, Z., Yu, J., Kotsia, I., and Zafeiriou, S. Retinaface: Single-stage dense face localisation in the wild. In *arxiv*, 2019.
- Diamond, S., Sitzmann, V., Julca-Aguilar, F., Boyd, S., Wetzstein, G., and Heide, F. Dirty pixels: Towards end-to-end image processing and perception. *ACM Transactions on Graphics (TOG)*, 40(3):1–15, 2021.
- Gaikwad, V. and Rake, R. Video analytics market statistics: 2027, 2021. URL <https://www.alliedmarketresearch.com/video-analytics-market>.
- Gupta, A., Anpalagan, A., Guan, L., and Khwaja, A. S. Deep learning for object detection and scene perception in self-driving cars: Survey, challenges, and open issues. *Array*, 10:100057, 2021. ISSN 2590-0056. doi: <https://doi.org/10.1016/j.array.2021.100057>. URL <https://www.sciencedirect.com/science/article/pii/S2590005621000059>.
- Hsieh, K., Ananthanarayanan, G., Bodik, P., Venkataraman, S., Bahl, P., Philipose, M., Gibbons, P. B., and Mutlu, O. Focus: Querying large video datasets with low latency and low cost. In *13th USENIX Symposium on Operating Systems Design and Implementation (OSDI 18)*, pp. 269–286, Carlsbad, CA, October 2018. USENIX Association. ISBN 978-1-939133-08-3. URL <https://www.usenix.org/conference/osdi18/presentation/hsieh>.
- i PRO. i-pro network camera. <http://i-pro.com/global/en/surveillance>.
- Jiang, J., Ananthanarayanan, G., Bodik, P., Sen, S., and Stoica, I. Chameleon: scalable adaptation of video analytics. In *Proceedings of the 2018 Conference of the ACM Special Interest Group on Data Communication*, pp. 253–266, 2018.
- Kang, D., Emmons, J., Abuzaid, F., Bailis, P., and Zaharia, M. Noscope: Optimizing neural network queries over video at scale. *Proc. VLDB Endow.*, 10(11):1586–1597, August 2017. ISSN 2150-8097. doi: 10.14778/3137628.



3137664. URL <https://doi.org/10.14778/3137628.3137664>.
- Khani, M., Hamadani, P., Nasr-Esfahany, A., and Alizadeh, M. Real-time video inference on edge devices via adaptive model streaming. *arXiv preprint arXiv:2006.06628*, 2020.
- Kingma, D. P. and Ba, J. Adam: A method for stochastic optimization. *arXiv preprint arXiv:1412.6980*, 2014.
- Krizhevsky, A., Sutskever, I., and Hinton, G. E. Imagenet classification with deep convolutional neural networks. In *Advances in neural information processing systems*, pp. 1097–1105, 2012.
- Kuehne, H., Jhuang, H., Garrote, E., Poggio, T., and Serre, T. HMDB: a large video database for human motion recognition. In *Proceedings of the International Conference on Computer Vision (ICCV)*, 2011.
- Li, Y., Padmanabhan, A., Zhao, P., Wang, Y., Xu, G. H., and Netravali, R. Reducto: On-camera filtering for resource-efficient real-time video analytics. In *Proceedings of the Annual conference of the ACM Special Interest Group on Data Communication on the applications, technologies, architectures, and protocols for computer communication*, pp. 359–376, 2020.
- Liu, L., Jia, X., Liu, J., and Tian, Q. Joint demosaicing and denoising with self guidance. In *Proceedings of the IEEE/CVF Conference on Computer Vision and Pattern Recognition*, pp. 2240–2249, 2020.
- Liu, Z., Luo, P., Wang, X., and Tang, X. Deep learning face attributes in the wild. In *Proceedings of International Conference on Computer Vision (ICCV)*, December 2015.
- Niebles, J. C., Chen, C.-W., and Fei-Fei, L. Modeling temporal structure of decomposable motion segments for activity classification. In *European conference on computer vision*, pp. 392–405. Springer, 2010.
- Nishimura, J., Gerasimow, T., Rao, S., Sutic, A., Wu, C.-T., and Michael, G. Automatic isp image quality tuning using non-linear optimization, 2019.
- opencvtoolkit. Computer vision annotation tool (cvat). <https://github.com/opencvtoolkit/cvat>.
- Padmanabhan, A., Iyer, A. P., Ananthanarayanan, G., Shu, Y., Karianakis, N., Xu, G. H., and Netravali, R. Towards memory-efficient inference in edge video analytics.
- Patrick Grother, M. N. and Hanaoka, K. Face Recognition Vendor Test (FRVT). <https://nvlpubs.nist.gov/nistpubs/ir/2019/NIST.IR.8271.pdf>, 2019.
- Paul, S., Drolia, U., Hu, Y. C., and Chakradhar, S. T. Aqua: Analytical quality assessment for optimizing video analytics systems, 2021.
- Qualcomm. How 5g low latency improves your mobile experiences. Qualcomm\_5G\_low\_latency\_improves\_mobile\_experience, 2019.
- Ramanath, R., Snyder, W. E., Yoo, Y., and Drew, M. S. Color image processing pipeline. *IEEE Signal Processing Magazine*, 22(1):34–43, 2005.
- Statisticssolutions. Pearson correlation coefficient. <https://www.statisticssolutions.com/free-resources/directory-of-statistical-analyses/pearsons-correlation-coefficient/>, 2019.
- Sutton, R. S., Barto, A. G., et al. *Introduction to reinforcement learning*, volume 135. MIT press Cambridge, 1998.
- Szegedy, C., Vanhoucke, V., Ioffe, S., Shlens, J., and Wojna, Z. Rethinking the inception architecture for computer vision. In *2016 IEEE Conference on Computer Vision and Pattern Recognition (CVPR)*, pp. 2818–2826, 2016. doi: 10.1109/CVPR.2016.308.
- Tan, M., Pang, R., and Le, Q. V. Efficientdet: Scalable and efficient object detection. In *Proceedings of the IEEE/CVF conference on computer vision and pattern recognition*, pp. 10781–10790, 2020.
- Watkins, C. J. C. H. and Dayan, P. Q-learning. In *Machine Learning*, pp. 279–292, 1992.
- Wiering, M. and Schmidhuber, J. Fast online  $q(\lambda)$ . *Machine Learning*, 33(1):105–115, Oct 1998. ISSN 1573-0565. doi: 10.1023/A:1007562800292. URL <https://doi.org/10.1023/A:1007562800292>.
- Wu, C.-T., Isikdogan, L. F., Rao, S., Nayak, B., Gerasimow, T., Sutic, A., Ain-kedem, L., and Michael, G. Visionisp: Repurposing the image signal processor for computer vision applications. In *2019 IEEE International Conference on Image Processing (ICIP)*, pp. 4624–4628. IEEE, 2019.
- Zhang, B., Jin, X., Ratnasamy, S., Wawrzyniak, J., and Lee, E. A. Awstream: Adaptive wide-area streaming analytics. In *Proceedings of the 2018 Conference of the ACM Special Interest Group on Data Communication*, pp. 236–252, 2018.
- Zhang, H., Ananthanarayanan, G., Bodik, P., Philipose, M., Bahl, P., and Freedman, M. J. Live video analytics at scale with approximation and delay-tolerance. In *14th USENIX Symposium on Networked Systems Design and Implementation (NSDI 17)*, pp. 377–392, Boston,

MA, March 2017. USENIX Association. ISBN 978-1-931971-37-9. URL <https://www.usenix.org/conference/nsdi17/technical-sessions/presentation/zhang>.